Published in final edited form as:
Cell Microbiol. 2008 August ; 10(8): 1695–1710. doi:10.1111/j.1462-5822.2008.01160.x.

Vesicular transport in *Histoplasma capsulatum*: an effective mechanism for trans-cell wall transfer of proteins and lipids in ascomycetes

Priscila Costa Albuquerque[1,2,3], **Ernesto S. Nakayasu**[4], **Marcio L. Rodrigues**[5], **Susana Frases**[2], **Arturo Casadevall**[2,3], **Rosely M. Zancope-Oliveira**[1], **Igor C. Almeida**[4], and **Joshua D. Nosanchuk**[2,3,*]

[1] Instituto de Pesquisa Clinica Evandro Chagas, Fundação Oswaldo Cruz, RJ Brazil

[2] Department of Microbiology and Immunology, Division of Infectious Diseases, Albert Einstein College of Medicine, Yeshiva University, New York, NY, USA

[3] Department of Medicine, Albert Einstein College of Medicine, Yeshiva University, New York, NY, USA

[4] Department of Biological Sciences, The Border Biomedical Research Center, University of Texas at El Paso, El Paso, TX,, USA

[5] Instituto de Microbiologia Professor Paulo de Góes, Universidade Federal do Rio de Janeiro, RJ Brazil

Abstract

Vesicular secretion of macromolecules has recently been described in the basidiomycete *Cryptococcus neoformans* raising the question as to whether ascomycetes similarly utilize vesicles for transport. In the present study, we examine whether the clinically important ascomycete *Histoplasma capsulatum* produce vesicles and utilized these structures to secrete macromolecules. Transmission electron microscopy (TEM) show transcellular secretion of vesicles by yeast cells. Proteomic and lipidomic analyses of vesicles isolated from culture supernatants reveals a rich collection of macromolecules involved in diverse processes including metabolism, cell recycling, signaling, and virulence. The results demonstrate that *H. capsulatum* can utilize a trans-cell wall vesicular transport secretory mechanism to promote virulence. Additionally, TEM of supernatants collected from *Candida albicans*, *Candida parapsilosis*, *Sporothrix schenckii*, and *Saccharomyces cerevisiae* document that vesicles are similarly produced by additional ascomycetes. The vesicles from *H. capsulatum* react with immune serum from patients with histoplasmosis providing an association of the vesicular products with pathogenesis. The findings support the proposal that vesicular secretion is a general mechanism in fungi for the transport of macromolecules related to virulence and that this process could be a target for novel therapeutics.

Keywords

Histoplasma capsulatum; ascomycete; vesicles; transcellular transport

*Corresponding author. Mailing address: Albert Einstein College of Medicine, 1300 Morris Park Ave., Bronx, NY 10461. Phone: 718 430-3659. Fax: 430-8701. E-mail: nosanchu@aecom.yu.edu.

Conflict of interest: The authors do not have any conflicts of interest.

Introduction

Histoplasma capsulatum, a dimorphic fungus of the phylum *Ascomycota*, is a major human pathogen with a worldwide distribution (Kauffman, 2007). The fungus usually causes a mild, often asymptomatic respiratory illness, but infection may progress to life-threatening systemic disease, particularly in immunocompromised individuals, infants, or the elderly. *H. capsulatum* grows as a saprophytic mould in the environment but undergoes phase transition to a yeast form at mammalian physiological temperatures. Within macrophages, *H. capsulatum* modifies its microenvironment over a broad pH range, survives nutrient-starvation, resists reactive oxygen and nitrogen species, and survives exposure to degradative enzymes (Woods, 2002). In the yeast form, several important exoantigens have been described, including the H and M antigens, pluripotent glycoproteins that elicit both humoral and T-cell-mediated immune responses (Deepe and Gibbons, 2001b; Fisher and Woods, 2000; Zancope-Oliveira *et al.*, 1999), and a virulence-related, phase specific protein (YPS3p), that is found at the cell wall (Bohse and Woods, 2007; Bohse and Woods, 2005). Yeast cells secrete a calcium-binding protein (CBP) that enables the fungus to grow in calcium-limiting conditions (Sebghati *et al.*, 2000). Heat shock proteins are also produced at a high level, which is consistent with the thermally dimorphic nature of the organism (Burnie *et al.*, 2006).

In contrast to prokaryotic organisms, secretory pathways in eukaryotic cells involve vesicular traffic of molecules to the plasma membrane (van Meer and Sprong, 2004; Ponnambalam and Baldwin, 2003). Fungal cells have complex cell walls and are therefore expected to require additional mechanisms to transfer periplasmic components from the plasma membrane to the extracellular space. The mechanisms by which macromolecules reach the extracellular environment and how they are transported through the cell wall, however, have not been rigorously explored in fungi. It has been recently described that the yeast-like pathogen *Cryptococcus neoformans* produces secretory vesicles that transport its major capsular polysaccharide to the extracellular space (Rodrigues *et al.*, 2008; Rodrigues *et al.*, 2007; Yoneda and Doering, 2006). The polysaccharide is synthesized intracellularly (Garcia-Rivera *et al.*, 2004; Feldmesser *et al.*, 2001) and packaged into lipid vesicles, which cross the cell wall and the capsule network by still unknown mechanisms to reach the extracellular environment. At the extracellular space, the polysaccharide is released and presumably used for capsule assembly (Rodrigues *et al.*, 2007). Furthermore, bioactive fungal lipids, including glucosylceramides and sterols, are secreted by *C. neoformans* vesicles (Rodrigues *et al.*, 2007). It remains unknown whether other pathogenic fungal species use the same mechanism to secrete extracellular molecules.

In the present study, we demonstrate that the parasitic yeast stage of *H. capsulatum* produces heterogeneous vesicles that are secreted extracellularly. A considerable variety of molecules, including phospholipids and proteins associated to stress responses, pathogenesis, cell wall architecture and virulence comprise the *H. capsulatum* vesicles. Furthermore, we analyzed whether additional ascomycetes, including *Candida albicans*, *Candida parapsilosis*, *Sporothrix schenckii* and *Saccharomyces cerevisiae*, produced vesicles. Finally, proteins extracted from *H. capsulatum* vesicles reacted with immune sera from patients with histoplasmosis suggesting that the vesicles are involved in host-pathogen interactions. These results show that vesicular secretion is a common mechanism of extracellular delivery in fungi.

Results

H. capsulatum produces extracellular vesicles

Extracellular vesicles were obtained from *H. capsulatum* yeast. Using our growth conditions, *H. capsulatum* is in exponential phase growth for the first 72–76 hours. At the time of collection, the yeast cells were >99% viable by propidium iodine staining, which makes the possibility of the vesicles arising from dead or dying cells exceedingly unlikely. TEM of the material recovered by ultracentrifugation of supernatants from *H. capsulatum* revealed the presence of bilayered, spherical vesicles (Fig. 1). Five hundred and eight vesicles were analyzed and were found to range in size from 10 to 350 nm (Fig. 2). The electron density of the vesicles varied considerably, suggesting distinct contents (Fig. 1). The protocol used for the isolation of *H. capsulatum* extracellular vesicles was based on that used for *C. neoformans* (Rodrigues *et al.*, 2007), in which organelles from dead cells were not found. Similarly, organelles were not found in culture supernatants of heat-killed *H. capsulatum* yeast cells examined by TEM (data not shown). Notably, we identified vesicular structures in internal and outer regions of the cell wall, as well as in the extracellular environment (Fig. 3), which is in accordance with the proposal that vesicle secretion is an active mechanism in living *H. capsulatum* cells. Vesicles were identified in and adjacent to the cell walls of all yeast cells analyzed (n = 200) indicating that this is a pervasive process.

Membrane phospholipids are present in vesicular lipid extracts

Lipids were fractioned and analyzed by ESI-MS, in negative or positive-ion mode. The regions of the spectra in which molecular masses corresponding to phospholipids were expected are presented in Figure 4. The major peaks observed in both spectra were subjected to MS/MS analysis (Supplemental Figure 1), resulting in the identification of 17 different phospholipids (Table 1). In the negative-ion mode analysis, only phosphatidylethanolamine (PE) species were detected as major phospholipid species (Fig 4, Table 1). As shown in the Supplemental Figure 1A–E, diagnostic ions for PE were found at *m/z* 140.1 and 196.1, corresponding to ethanolamine phosphate (EtNP) and dehydrated glyceroethanolaminephosphate (GroEtNP/H_2O), respectively. Fragment ions corresponding to the carboxylate ions of the acyl chains were also detected. On the other hand, the positive-ion mode analysis revealed mainly PE, phosphatidylserine (PS), and phosphatidylcholine (PC) as the major phospholipid species (Table 1, Supplemental Figure 1F-P). MS/MS spectra of PE species revealed diagnostic ions corresponding to the presence of cyclic ethanolaminephosphate ($EtNP_c$) plus 2 Li+ adducts (*m/z* 152.0), and the neutral losses of ethanolamine (EtN) and ethanolaminephosphate (EtNP). MS/MS spectra of PC species were characterized by the presence of the diagnostic ion choline (Cho) at *m/z* 86.0, and neutral losses of trimethylamine (Me_3N) and phosphocholine (ChoP). Finally, MS/MS spectra of PS species were characterized by the presence of dehydrated serinephosphate (SerP - H_2O) and serinephosphate (SerP) ion species at *m/z* 168.0 and 186.0, respectively. The neutral loss of carboxyl group from Ser was also detected in most PS species (Supplemental Figure 1). For all phospholipid species analyzed in the positive-ion mode, the composition of acyl chains was determined by the neutral loss of these structures. In sum, PE and PC, followed by PS, were the most abundant phospholipids found in the MS analyses, consistent with the typical lipid distribution in pathogenic yeasts (Rattray *et al.*, 1975).

Proteomic analysis of the *H. capsulatum* extracellular vesicles

After vesicle purification, proteins were enzymatically digested and resulting peptides were fractionated by cation exchange chromatography and analyzed by liquid chromatography-tandem mass spectrometry (LC-MS/MS). All generated MS/MS spectra were searched against a database assembled with *H. capsulatum* predicted sequences and randomly generated sequences. After estimating the false-positive rate (FPR), 283 proteins were

validated and 206 identified by sequence analysis. Table 2 summarizes the identified proteins with associated biological function(s). A comprehensive list of all identified proteins and detailed parameters of the LC-MS/MS analysis are provided in Supplemental Table 1. Some of these proteins, such as chaperones (Hsp70, Hsp30, and Hsp60 precursors), superoxide dismutase, and catalase B, are involved in *H. capsulatum* pathogenesis and host immune responses. Others (e.g., Rab GDP-dissociation inhibitor, Rab1a, GTP-binding nuclear protein GSP1/Ran) are involved in signal transduction pathways and vesicle formation. We also identified several proteins implicated in cell wall architecture, cell growth, sugar, lipid, and amino acid metabolism, as well as cytoskeleton-related proteins. Several peroxisomal, nuclear, proteasomal, and ribosomal proteins and proteins with additional localization/function were also identified. Many of these proteins were recently described in the proteome of vesicles from *C. neoformans* (Rodrigues *et al.*, 2008) as well as in mammalian vesicles (Aoki *et al.*, 2007;Potolicchio *et al.*, 2005). Table 3 shows the distribution of the identified *H. capsulatum* vesicle proteins according to their functions.

TEM of *C. albicans, C. parapsilosis, S. schenckii,* and *S. cerevisiae* vesicles

TEM of the material recovered by ultracentrifugation from culture supernatants of *C. albicans, C. parapsilosis, S. schenckii* and *S. cerevisiae* revealed that other ascomycetes similarly produce extracellular vesicles (Fig. 5). The structures identified were similar to vesicles produced by *C. neoformans* (Rodrigues *et al.*, 2008;Rodrigues *et al.*, 2007) and *H. capsulatum*, consisting of bilayered membranes and largely spherical morphologies. Although significant differences in size were found for the ascomycetes studied, they all predominantly produced vesicles ≤ 50 nm in diameter. Only 4% of *S. cerevisiae* vesicles were larger than 50 nm though none were more than 100 nm in diameter. For *S. schenckii*, 11% were between 51–100 nm, but none were larger. For *C. albicans* and *C. parapsilosis*, 13% and 36% of vesicles were 50–100 nm, respectively. Vesicles larger than 100 nm comprised 1% and 18% of total vesicles for *C. albicans* and *C. parapsilosis*, respectively.

Sera of patients recognized proteins from the vesicles

Pooled sera from patients with histoplasmosis were used in immunoblots against protein extracts of *H. capsulatum* (Fig. 6). Extracts of *H. capsulatum* vesicles reacted with serum from patients with histoplasmosis. Immunogenic proteins with diverse molecular masses were observed (Figure 6 B). To confirm the identification of certain proteins identified in the proteomic analysis for which reagents for *H. capsulatum* are available, immunoblots were performed with mAbs to histone 2B and heat shock protein 60 (Figure 6 D and E, respectively). The identified bands corresponded to bands recognized by the pooled histoplasmosis sera. These proteins were identified in the proteomic analysis described above. Non-immune sera did not react with proteins from the vesicles (Figure 6 C).

Discussion

We recently showed that secretory vesicles are involved in the extracellular release of virulence determinants in the fungal pathogen *C. neoformans* (Rodrigues *et al.*, 2008; Rodrigues *et al.*, 2007). We now describe that *H. capsulatum, C. albicans, C. parapsilosis, S. schenckii* and *S. cerevisiae* also produce extracellular vesicles. Furthermore, we show that *H. capsulatum* produces vesicles containing key molecules related to virulence, stress response and fungal physiology. By microscopic and mass spectrometric approaches, *H. capsulatum* vesicles were identified as lipid bodies with bilayered membrane containing proteins of diverse functions and a number of phospholipids. The findings of this study, combined with the recent reports on *C. neoformans* (Rodrigues *et al.*, 2008; Rodrigues *et al.*, 2007; Yoneda and Doering, 2006; Garcia-Rivera *et al.*, 2004; Feldmesser *et al.*, 2001),

indicate that vesicular secretion is an important mechanism for fungi to deliver intracellular molecules to the extracellular space.

For *H. capsulatum*, vesicular bodies were observed in association with the cell wall and in the extracellular environment, suggesting the active use of vesicular transport for secretory processes. Microscopic analysis of the samples obtained after differential centrifugation of culture supernatants revealed intact vesicles ranging in size from approximately 10 to 350 nm (Fig 2). Despite this heterogeneity, the vesicles all had an ovoid appearance and displayed lipid bilayered membranes. Differences in electron density were observed, suggesting heterogeneity in vesicular contents (Fig. 1). Vesicles were not released from dead cells and the yeast were studied in log phase growth during which there is negligible cell death.

C. albicans continues to be the leading opportunistic pathogen involved in oral, vaginal, and systemic infections resulting in high mortality, and *Candida spp.* are the fourth most common cause of bloodstream infection in the United States (Wisplinghoff *et al.*, 2004). *C. parapsilosis* is currently the second most common cause of invasive candidiasis worldwide (Fridkin *et al.*, 2006) and is particularly associated with disease in premature infants, immunocompromised adults, and patients in intensive care units (Clerihew *et al.*, 2007). The dimorphic fungus *S. schenckii* has a worldwide distribution and causes disease primarily after traumatic inoculation of colonized materials and less commonly by inhalation of spores through the respiratory tract (Almeida-Paes *et al.*, 2007a). Rarely pathogenic, *S. cerevisiae* is a well-established model organism for understanding fundamental cellular processes relevant to higher eukaryotic organisms (Botstein and Fink, 1988). Microscopic analysis of the additional fungal species studied revealed intact vesicles of varied morphology, yet the vesicles shared a common ovoid appearance and all displayed lipid bilayered membranes. Interestingly, vesicular transport has been proposed previously in *C. albicans* in an opaque variant of strain WO-1 in which electron microscopy analysis of intact cells revealed “pimples” in the cell wall with vesicles within channels or emerging from the “pimples” (Anderson *et al.*, 1990). Future studies are required to assess the contents of the vesicles produced by these ascomycetes, and it will be imperative to assess whether vesicles of different sizes transport specific compounds. For instance, it will be important to determine whether virulence associated products (ie. heat shock proteins, catalases, superoxide dismutases, etc) are transported in the larger vesicles previously described in *C. neoformans* (Rodrigues *et al.*, 2008) and herein identified for *Candida spp.* and *H. capsulatum* but are lacking in the smaller vesicles of less pathogenic fungi such as *S. cerevisiae*.

In our analyses of *H. capsulatum* vesicles, phospholipids were characterized as lipid components of vesicle membranes. The major phospholipids found were PC, PE and PS, which are building blocks for cellular membranes (lipid bilayers). These lipids also perform a diverse number of other functions, from compartmentalization of cytoplasm to the housing of proteins involved in cell signaling, intercellular adhesion, and cytoskeletal support (16). Previous studies have shown that cell communication might not be limited to soluble agonists, but that various types of vesicles also participate in the process (Denzer *et al.*, 2000). It is notable that mammalian exosome membranes display a similar content of phospholipids and are also formed as lipid bilayers with a random distribution analogous to *H. capsulatum* vesicle phospholipids (Laulagnier *et al.*, 2004). Hence, this similarity to mammalian exosomes supports the supposition that the vesicles from *H. capsulatum* are exosome-like structures. Exosomes are part of the family of bioactive vesicles and appear to be involved in distal communications between cells. They transport bioactive lipids and lipolytic enzymes and their biogenesis requires specific lipids and membrane reorganization (Subra *et al.*, 2007). Bioactive vesicles are receiving increasing interest since they are important in enhancing biodiversity and are the only type of bioactive vesicles originating

from intracellular compartments, namely multi-vesicular bodies (MVBs, or late endosomes) (Fevrier and Raposo, 2004). MVBs participate in the eradication of obsolete proteins, but they can also be released into extracellular space where they can potentially affect intercellular communication (van Niel *et al.*, 2006).

We used a proteomics approach to analyze the protein contents of vesicles. *H. capsulatum* survives and replicates within host macrophages (Allendoerfer and Deepe, 1997), denoting the necessity of fungal mechanisms to escape the antimicrobial armory of phagocytes. The secretion of virulence factors is a mechanism used by different pathogens to cause damage to host cells. In this context, the presence of anti-oxidant proteins in secreted vesicles, such as catalase B (M antigen) (Zancope-Oliveira *et al.*, 1999), superoxide dismutase precursors (Brummer and Stevens, 1995), and a thiol-specific antioxidant protein (Demasi *et al.*, 2006), could represent an effective mechanism of fungal defense. The proteomic analysis of the *H. capsulatum* vesicles identified proteins involved in vesicular transport and fusion, especially proteins from the Rab family. In mammals, Rabs define a family of almost 70 proteins that play critical roles in the trafficking of vesicles that mediate transport between compartments of the exocytic and endocytic pathways (Pfeffer, 2005; Pfeffer, 2001). Several of the identified *H. capsulatum* Rab proteins have been characterized to have similar functions, such as *H. capsulatum* Rab GDP-dissociation inhibitor that plays a key role in the recycling of Rabs (Ma *et al.*, 2006)and *H. capsulatum* Rab1a that regulates antegrade transport between the ER and the Golgi apparatus (Sannerud *et al.*, 2006). The presence of *H. capsulatum* endochitinase and glucanases in the vesicles is also consistent, since these molecules are membrane proteins and the vesicles may originate from membrane invagination, similar to exosome formation (Sannerud *et al.*, 2006). The mechanisms by which fungal vesicles traverse the cell wall are still unknown. In this context, the existence of vesicular enzymes with the ability to hydrolyze cell wall components is particularly interesting, since these molecules have the potential to promote cell wall reassembly for vesicle passage.

The extracellular *H. capsulatum* vesicles also contained chaperone and nucleus-associated proteins. Several heat-shock proteins were present in the vesicles. *H. capsulatum* Hsp60 is particularly noteworthy since this immunodominant molecule is key to the engagement of the yeast with CD18 receptors on host macrophage (Long *et al.*, 2003) and vaccination with this protein is protective (Gomez *et al.*, 1995). *H. capsulatum* Hsp70 is also immunogenic, though it induces non-protective cellular responses (Allendoerfer *et al.*, 1996). *H. capsulatum* nuclear proteins, such as H2B, can be displayed on the fungal cell surface where they can be targeted by antifungal antibodies (Nosanchuk *et al.*, 2003). An *H. capsulatum* glyceraldehyde-3-phosphate dehydrogenase was also identified and a homologous protein is present in the cell wall of the fungal pathogen *Paracoccidioides brasiliensis*, where it mediates the adhesion of yeast cells to host cells and extracellular matrixes (Barbosa *et al.*, 2006). These examples of single proteins with multiple activities are consistent with the emerging understanding that many proteins have ‘moonlighting’ functions enabling cells to efficiently perform diverse tasks despite limited genomes (Jeffery, 2003b; Jeffery, 2003a; Jeffery, 1999). Moonlighting proteins described from *S. cerevisiae* to humans have included enzymes, chaperones, ribosomal protein, receptors, and transmembrane channels.

In order to assess whether vesicles have a biological effect on the host, we tested the immunoreactivity of extracted vesicular proteins with patients’ sera. The recognition of diverse proteins by pooled hyperimmune patient sera indicates that these vesicularly transported proteins could be important in the pathogenesis of these mycoses. For example heat shock protein 60 from *H. capsulatum* has been associated with virulence (Deepe and Gibbons, 2002; Scheckelhoff and Deepe, 2002; Deepe and Gibbons, 2001a; Allendoerfer *et*

al., 1996; Gomez *et al.*, 1995). The findings are consistent with vesicular transport playing a role in host-pathogen interactions.

In summary, we report the trans-cell wall vesicular transport of several important components of virulence, signaling and recycling in *H. capsulatum.* The vesicles appear to be similar to mammalian exosomes. We also show that other ascomycetes produce vesicles that can function in the transport of macromolecules. The products of the vesicles are immunoreactive with serum from patients, which supports our hypothesis that the vesicles are involved in fungal pathogenesis. Hence, we propose that fungal extracellular vesicle secretion is an important mechanism in fungal biology.

Materials and Methods

Fungal strains and growth conditions

H. capsulatum strain G217B (ATCC 26032) was obtained from the American Type Culture Collection (ATCC, Rockville, Maryland, USA). G217B yeast cells were grown in 500 mL Ham's F-12 medium with rotary shaking (150 rpm) at 37 °C for 48 h in Erlenmeyer flasks as described previously (Nosanchuk *et al.*, 2003). Thimerosal- and heat-killed *H. capsulatum* yeast cells were used as a negative control. *Candida albicans* SC5314 (ATCC MYA-2876 (Gillum *et al.*, 1984)), *Candida parapsilosis* strain GA1 (a clinical isolate (Gacser *et al.*, 2005)) and *S. schenckii* strain 23508 (a clinical isolate (Almeida-Paes *et al.*, 2007b)) were grown in Sabouraud dextrose broth (Difco Laboratories, Detroit, MI) with rotary shaking (150 rpm) at 30°C for 48 hours for *Candida spp.* or at 37°C for 3 days in the case of *S. schenckii. S. cerevisiae* strain KFY 471 (BY4741; ATTC 201388 (Winzeler *et al.*, 1999)) was provided by Dr. Michael Keogh (Albert Einstein, New York), and was grown in YPD broth (Difco Laboratories, Detroit, MI) in the same conditions used for *Candida* strains.

Isolation of vesicles

Vesicle isolation was performed according to our previously described protocol (Rodrigues *et al.*, 2007). Briefly, the fungal cells were separated from culture supernatants by centrifugation at 4,000 g for 15 min at 4°C. Supernatants were collected and again centrifuged at 15,000 g (4°C) for 30 min to remove smaller debris. The pellets were discarded, and the resulting supernatant was concentrated approximately 20-fold using an Amicon ultrafiltration system (cutoff, 100 kDa). To ensure the removal of cells and cellular debris, the concentrated culture fluid was again centrifuged as described above and the resulting supernatant was then centrifuged at 100,000 g for 1 h at 4°C. The supernatants were discarded and the pellets suspended in 3 mL of 0.1 M Phosphate-buffered saline (PBS) and centrifuged at 100,000 g for 1 h at 4°C. The supernatant was again removed from the pellets and a fixative solution (as described below), was added for electron microscopy analysis. Additionally, pellets from *H. capsulatum* were used for proteomic analysis or extracted with a chloroform-methanol mixture for lipidomic analysis as described below.

Transmission electron microscopy (TEM)

TEM was used to visualize vesicles in intact *H. capsulatum* yeast cells and vesicles isolated from culture supernatants of *H. capsulatum* and the other fungi by ultracentrifugation. Samples were fixed in 2.5% glutaraldehyde in 0.1 M cacodylate buffer at room temperature for 2 h and then incubated overnight in 4% paraformaldehyde, 1% glutaraldehyde, and 0.1% phosphate-buffered saline (PBS). The samples were incubated for 90 min in 2% osmium tetroxide, serially dehydrated in ethanol, and embedded in Spurr's epoxy resin. Thin sections were obtained on a Reichert Ultracut and stained with 0.5% uranyl acetate and 0.5% lead citrate. Samples were observed in a JEOL 1200EX transmission electron microscope operating at 80 kV.

Mass spectrometry analysis of phospholipids

The *H. capsulatum* vesicle fraction was suspended in 100 μL of ultrapure water and extracted 3x by addition of 1.5 ml chloroform:methanol (2:1, v/v) solution followed by vigorous vortexing and then centrifugation for 10 min at 1000 g. After drying under nitrogen stream, the sample was dissolved in 500 μL chloroform and loaded onto a silica gel 60 column, equilibrated with pure chloroform. The silica column was manufactured in a Pasteur pipette, using a very fine glass wool and about 500 mg of silica gel 60 resin (pore size 60 Å, 200–400 μm mesh) (Sigma-Aldrich, St. Louis. MO). After washing the column with chloroform, followed by acetone, the phospholipids were eluted with methanol and dried under nitrogen stream. The phospholipid fraction was dissolved in chloroform:methanol (1:1, v/v) and diluted either in chloroform:methanol (1:1, v/v) containing 10 mM LiOH (for positive-ion mode analysis) or chloroform:methanol (1:1, v/v) containing 0.1% formic acid (FA) and 0.1% NH_4OH (for negative-ion mode analysis), and analyzed in an electrospray ionization time-of-flight mass spectrometer (ESI-Q-TOF-MS) (Qtof-1, Waters). The spectra were collected in a range from 400 to 1500 *m/z* and each ion with intensity higher than 10 counts was automatically submitted to collision-induced dissociation (CID) (22–60 eV, 50–1500 *m/z* range). MS/MS spectra were analyzed manually for the identification of phospholipid species.

Protein identification by liquid chromatography tandem mass spectrometry

Protein digestion was performed as described previously (Stone and Williams, 1996). Purified vesicles were suspended in 40 μl 400 mM NH_4HCO_3 containing 8 M urea and the protein disulfide bounds were reduced by the addition of 10 μl 50 mM dithiotreitol for 15 min at 50°C. Cysteine residues were alkylated by the addition of 10 μl 100 mM iodoacetamide and incubation for an additional 15 min at room temperature protected from light. The reaction was diluted with HPLC-grade water (Sigma-Aldrich) to obtain a final concentration of 1 M urea, and the digestion was performed overnight at 37°C with 4 μg sequencing-grade trypsin (Promega). Each sample was desalted in a reverse phase ziptip (POROS R2 50, Applied Biosystems) as described by Jurado et al. (Jurado *et al.*, 2007), and peptides were fractionated in a strong cation-exchange (SCX) ziptip, manufactured in a 200-μl micropipette tip with glass fiber filter and POROS HS 50 resin (Applied Biosystems). After equilibrating the SCX ziptip with 25% acetonitrile (ACN)/0.5% FA, peptides were loaded and eluted with increasing NaCl concentration (0, 10, 20, 40, 60, 80, 100, 150, 200, and 500 mM NaCl in 25% ACN/0.5% FA). Each SCX fraction was dried in a vacuum centrifuge (Eppendorf), purified in POROS R2 50 ziptip and redissolved in 30 μl 0.05% trifluoroacetic acid (TFA). Eight μl of fractionated peptides were loaded onto a C18 trap column (1 yL C18, OPTI-PAK) and washed for 10 min with 2% ACN/0.1% FA. The separation was performed in a capillary reverse-phase column (Acclaim, 3 μm C18, 75 μm x 25 cm, LC Packings) connected to a nanoHPLC system (nanoLC 1D plus, Eksigent). Peptides were eluted in a 0–40% gradient of solvent B (solvent A: 2%ACN/0.1%FA, solvent B: 80%ACN/0.1% FA) during 100 min and directly analyzed in an electrospray ionization-linear ion trap-mass spectrometer (ESI-LIT-MS) equipped with a nanospray source (LTQ XL, Thermo Fisher Scientific, San Jose CA). MS spectra were collected in centroid mode in a range from 400 to 1700 *m/z* and the five most abundant ions were submitted twice to CID (35% normalized collision energy), before they were dynamically excluded for 120 sec.

All MS/MS spectra were obtained from peptides with 600–3500 Da and at least 15 fragments were converted into DTA files using Bioworks v.3.3.1 (Thermo Fisher Scientific). The DTA files were subjected to a database search using TurboSequest (Eng et al., 1994) (available in Bioworks software) against a database assembled with *H. capsulatum* (protein database, version of 05/11/2006, available at http://www.broad.mit.edu/annotation/genome/histoplasma_capsulatum/

Downloads.html;jsessionid=A347F284A23BE3CC423191220E09A48D), common contaminant sequences (retrieved from GenBank -http://www.ncbi.nlm.nih.gov/ and International Protein Index -http://www.ebi.ac.uk/IPI) and 100,000 randomly generated sequences. The database search parameters were: trypsin cleavage in both peptide termini with allowance for one missed cleavage site, carbamidomethylation of cysteine residues as a fixed modification, oxidation of methionine residues as a variable modification, and 2.0 Da and 1.0 Da for peptide and fragment mass tolerance, respectively. To ensure the quality of our identifications, we estimated the false-positive rate (FPR) from the TurboSequest output. This estimation was done using the following formula:

$$\mathrm{FPR}=\frac{\text{Mumber of protiens matching random sequences}}{\text{Total number of protiens}}$$

A FPR was obtained after applying the following filters in Bioworks: distinct peptides, consensus score ≥ 10.1, DCn ≥ 0.1, protein probability ≤ 1×10^{-3}, and Xcorr ≥ 1.5, 2.2, and 2.7 for singly-, doubly-, and triply-charged peptides, respectively. Using these parameters, the FPR was estimated as 3.7%.

Western Blot Analysis

H. capsulatum vesicles pellets were subjected to acetone precipitation. The precipitate was separated by sodium dodecyl sulfate-polyacrylamide gel electrophoresis (SDS-PAGE) using 10% gels. Separated proteins were transferred to nitrocellulose membranes and blocked (1% BSA in 0.1M PBS) for 1 h at 37°C. The membranes were then incubated in the presence of pooled sera from patients with culture proven histoplasmosis (Fiocruz- IPEC). Positive reactions were observed after incubation of blotted proteins with alkaline phosphatase-conjugated goat anti-human antibodies in blocking buffer for 1 h at 37°C followed by development with NBT-BCIP. Alternatively, the membranes were blocked and then incubated with monoclonal antibody to H2B (Nosanchuk *et al.*, 2003) or heat shock protein 60 (Guimarães *et al.*, 2006), washed in TBST, and incubated with goat anti-mouse Ig conjugated to horse raddish peroxidase. The samples were developed with ECL substrate (SuperSignal; Pierce Chemical Co.) and exposed on X-Omat AR film (Eastman Kodak Co., Rochester, New York, USA).

Supplementary Material

Refer to Web version on PubMed Central for supplementary material.

Acknowledgments

PCA was supported in part by an Interhemispheric Research Training Grant in Infectious Diseases, Fogarty International Center (NIH D43-TW007129). JDN is supported by NIH AI52733 and AI056070-01A2, and the Einstein MMC Center for AIDS Research [NIH NIAID AI51519]. MLR is supported by grants from the Brazilian agencies FAPERJ, CNPq and CAPES. R.M.Z.-O. is in part supported by CNPq 306288/2006-0 and by a grant from FAPERJ 306288/2006-0. AC is supported by NIH grants AI033142, AI033774, AI052733, and HL059842. ICA is supported by NIH grant 5G12RR008124 to the Border Biomedical Research Center (BBRC)/University of Texas at El Paso (UTEP). We are thankful to the Biomolecule Analysis Core Facility/BBRC/UTEP, supported by NIH/NCRR grant 5G12RR008124, for the use of the LC-MS instruments. The authors thank Dr. Fabio Gozzo (Laboratório Nacional de Luz Sincrontron, Campinas, Brazil) for kindly providing the 100,000 randomly generated sequences and Dr. Michael Keogh for providing the *S. cerevisiae* strain.

We also acknowledge that JE McEwen and CH Johnson postulated during the ASM Conference on Dimorphic Fungal Pathogens (Denver, Colorado, March 2006) that vesicles may be produced by *H. capsulatum.*

References

Allendoerfer R, Deepe GS Jr. Intrapulmonary response to *Histoplasma capsulatum* in gamma interferon knockout mice. Infect Immun. 1997; 65:2564–2569. [PubMed: 9199420]

Allendoerfer R, Maresca B, Deepe GS Jr. Cellular immune responses to recombinant heat shock protein 70 from *Histoplasma capsulatum*. Infect Immun. 1996; 64:4123–4128. [PubMed: 8926078]

Almeida-Paes R, Pimenta MA, Monteiro PC, Nosanchuk JD, Zancope-Oliveira RM. Immunoglobulins G, M and A against *Sporothrix schenckii* exoantigens in patients with sporotrichosis before and during treatment with itraconazole. Clin Vaccine Immunol. 2007a; 14:1149–1157. [PubMed: 17634504]

Almeida-Paes R, Pimenta MA, Pizzini CV, Monteiro PC, Peralta JM, Nosanchuk JD, Zancope-Oliveira RM. Use of mycelial-phase *Sporothrix schenckii* exoantigens in an enzyme-linked immunosorbent assay for diagnosis of sporotrichosis by antibody detection. Clin Vaccine Immunol. 2007b; 14:244–249. [PubMed: 17215334]

Anderson J, Mihalik R, Soll DR. Ultrastructure and antigenicity of the unique cell wall pimple of the *Candida* opaque phenotype. J Bacteriol. 1990; 172:224–235. [PubMed: 2403540]

Aoki N, Jin-no S, Nakagawa Y, Asai N, Arakawa E, Tamura N, et al. Identification and characterization of microvesicles secreted by 3T3-L1 adipocytes: redox- and hormone-dependent induction of milk fat globule-epidermal growth factor 8-associated microvesicles. Endocrinology. 2007; 148:3850–3862. [PubMed: 17478559]

Barbosa MS, Bao SN, Andreotti PF, de Faria FP, Felipe MS, dos Santos Feitosa L, et al. Glyceraldehyde-3-phosphate dehydrogenase of *Paracoccidioides brasiliensis* is a cell surface protein involved in fungal adhesion to extracellular matrix proteins and interaction with cells. Infect Immun. 2006; 74:382–389. [PubMed: 16368993]

Bohse ML, Woods JP. Surface localization of the Yps3p protein of Histoplasma capsulatum. Eukaryot Cell. 2005; 4:685–693. [PubMed: 15821128]

Bohse ML, Woods JP. RNA interference-mediated silencing of the YPS3 gene of *Histoplasma capsulatum* reveals virulence defects. Infect Immun. 2007; 75:2811–2817. [PubMed: 17403872]

Botstein D, Fink GR. Yeast: an experimental organism for modern biology. Science. 1988; 240:1439–1443. [PubMed: 3287619]

Brummer E, Stevens DA. Antifungal mechanisms of activated murine bronchoalveolar or peritoneal macrophages for Histoplasma capsulatum. Clin Exp Immunol. 1995; 102:65–70. [PubMed: 7554402]

Burnie JP, Carter TL, Hodgetts SJ, Matthews RC. Fungal heat-shock proteins in human disease. FEMS Microbiol Rev. 2006; 30:53–88. [PubMed: 16438680]

Clerihew L, Lamagni TL, Brocklehurst P, McGuire W. *Candida parapsilosis* infection in very low birthweight infants. Arch Dis Child Fetal Neonatal Ed. 2007; 92:F127–129. [PubMed: 17337658]

Deepe GS Jr, Gibbons R. V beta 6+ T cells are obligatory for vaccine-induced immunity to Histoplasma capsulatum. J Immunol. 2001a; 167:2219–2226. [PubMed: 11490008]

Deepe GS Jr, Gibbons R. Protective efficacy of H antigen from *Histoplasma capsulatum* in a murine model of pulmonary histoplasmosis. Infect Immun. 2001b; 69:3128–3134. [PubMed: 11292732]

Deepe GS Jr, Gibbons RS. Cellular and molecular regulation of vaccination with heat shock protein 60 from *Histoplasma capsulatum*. Infect Immun. 2002; 70:3759–3767. [PubMed: 12065519]

Demasi AP, Pereira GA, Netto LE. Yeast oxidative stress response. Influences of cytosolic thioredoxin peroxidase I and of the mitochondrial functional state. Febs J. 2006; 273:805–816. [PubMed: 16441666]

Denzer K, Kleijmeer MJ, Heijnen HF, Stoorvogel W, Geuze HJ. Exosome: from internal vesicle of the multivesicular body to intercellular signaling device. J Cell Sci. 2000; 113 Pt 19:3365–3374. [PubMed: 10984428]

Feldmesser M, Kress Y, Casadevall A. Dynamic changes in the morphology of *Cryptococcus neoformans* during murine pulmonary infection. Microbiology. 2001; 147:2355–2365. [PubMed: 11496012]

Fevrier B, Raposo G. Exosomes: endosomal-derived vesicles shipping extracellular messages. Curr Opin Cell Biol. 2004; 16:415–421. [PubMed: 15261674]

Fisher KL, Woods JP. Determination of beta-glucosidase enzymatic function of the *Histoplasma capsulatum* H antigen using a native expression system. Gene. 2000; 247:191–197. [PubMed: 10773459]

Fridkin SK, Kaufman D, Edwards JR, Shetty S, Horan T. Changing incidence of Candida bloodstream infections among NICU patients in the United States: 1995–2004. Pediatrics. 2006; 117:1680–1687. [PubMed: 16651324]

Gacser A, Salomon S, Schafer W. Direct transformation of a clinical isolate of *Candida parapsilosis* using a dominant selection marker. FEMS Microbiol Lett. 2005; 245:117–121. [PubMed: 15796988]

Garcia-Rivera J, Chang YC, Kwon-Chung KJ, Casadevall A. *Cryptococcus neoformans* CAP59 (or Cap59p) is involved in the extracellular trafficking of capsular glucuronoxylomannan. Eukaryot Cell. 2004; 3:385–392. [PubMed: 15075268]

Gillum AM, Tsay EY, Kirsch DR. Isolation of the *Candida albicans* gene for orotidine-5′-phosphate decarboxylase by complementation of S. cerevisiae ura3 and E. coli pyrF mutations. Mol Gen Genet. 1984; 198:179–182. [PubMed: 6394964]

Gomez FJ, Allendoerfer R, Deepe GS Jr. Vaccination with recombinant heat shock protein 60 from *Histoplasma capsulatum* protects mice against pulmonary histoplasmosis. Infect Immun. 1995; 63:2587–2595. [PubMed: 7790073]

Guimarães, AJ.; Williams, DA.; Zancope-Oliveira, RM.; Nosanchuk, JD. Protective antibodies to *Histoplasma capsulatum* cell surface antigens: heat shock protein 60 and M antigen (Abstract B35). ASM Conference on Dimorphic Fungal Pathogens; Denver, CO, ASM. 2006. p. 42

Jeffery CJ. Moonlighting proteins. Trends Biochem Sci. 1999; 24:8–11. [PubMed: 10087914]

Jeffery CJ. Multifunctional proteins: examples of gene sharing. Ann Med. 2003a; 35:28–35. [PubMed: 12693610]

Jeffery CJ. Moonlighting proteins: old proteins learning new tricks. Trends Genet. 2003b; 19:415–417. [PubMed: 12902157]

Jurado JD, Rael ED, Lieb CS, Nakayasu E, Hayes WK, Bush SP, Ross JA. Complement inactivating proteins and intraspecies venom variation in *Crotalus oreganus helleri*. Toxicon. 2007; 49:339–350. [PubMed: 17134729]

Kauffman CA. Histoplasmosis: a clinical and laboratory update. Clin Microbiol Rev. 2007; 20:115–132. [PubMed: 17223625]

Laulagnier K, Motta C, Hamdi S, Roy S, Fauvelle F, Pageaux JF, et al. Mast cell- and dendritic cell-derived exosomes display a specific lipid composition and an unusual membrane organization. Biochem J. 2004; 380:161–171. [PubMed: 14965343]

Long KH, Gomez FJ, Morris RE, Newman SL. Identification of heat shock protein 60 as the ligand on Histoplasma capsulatum that mediates binding to CD18 receptors on human macrophages. J Immunol. 2003; 170:487–494. [PubMed: 12496435]

Ma Y, Kuno T, Kita A, Nabata T, Uno S, Sugiura R. Genetic evidence for phospholipid-mediated regulation of the Rab GDP-dissociation inhibitor in fission yeast. Genetics. 2006; 174:1259–1271. [PubMed: 16980382]

Nosanchuk JD, Steenbergen JN, Shi L, Deepe GS Jr, Casadevall A. Antibodies to a cell surface histone-like protein protect against *Histoplasma capsulatum*. J Clin Invest. 2003; 112:1164–1175. [PubMed: 14561701]

Pfeffer S. A model for Rab GTPase localization. Biochem Soc Trans. 2005; 33:627–630. [PubMed: 16042559]

Pfeffer SR. Rab GTPases: specifying and deciphering organelle identity and function. Trends Cell Biol. 2001; 11:487–491. [PubMed: 11719054]

Ponnambalam S, Baldwin SA. Constitutive protein secretion from the trans-Golgi network to the plasma membrane. Mol Membr Biol. 2003; 20:129–139. [PubMed: 12851070]

Potolicchio I, Carven GJ, Xu X, Stipp C, Riese RJ, Stern LJ, Santambrogio L. Proteomic analysis of microglia-derived exosomes: metabolic role of the aminopeptidase CD13 in neuropeptide catabolism. J Immunol. 2005; 175:2237–2243. [PubMed: 16081791]

Rattray JB, Schibeci A, Kidby DK. Lipids of yeasts. Bacteriol Rev. 1975; 39:197–231. [PubMed: 240350]

Rodrigues ML, Nakayasu ES, Oliveira DL, Nimrichter L, Nosanchuk JD, Almeida IC, Casadevall A. Extracellular vesicles produced by *Cryptococcus neoformans* contain protein components associated with virulence. Eukaryot Cell. 2008; 7:58–67. [PubMed: 18039940]

Rodrigues ML, Nimrichter L, Oliveira DL, Frases S, Miranda K, Zaragoza O, et al. Vesicular polysaccharide export in *Cryptococcus neoformans* is a eukaryotic solution to the problem of fungal trans-cell wall transport. Eukaryot Cell. 2007; 6:48–59. [PubMed: 17114598]

Sannerud R, Marie M, Nizak C, Dale HA, Pernet-Gallay K, Perez F, et al. Rab1 defines a novel pathway connecting the pre-Golgi intermediate compartment with the cell periphery. Mol Biol Cell. 2006; 17:1514–1526. [PubMed: 16421253]

Scheckelhoff M, Deepe GS Jr. The protective immune response to heat shock protein 60 of *Histoplasma capsulatum* is mediated by a subset of V beta 8.1/8.2+ T cells. J Immunol. 2002; 169:5818–5826. [PubMed: 12421963]

Sebghati TS, Engle JT, Goldman WE. Intracellular parasitism by *Histoplasma capsulatum*: fungal virulence and calcium dependence. Science. 2000; 290:1368–1372. [PubMed: 11082066]

Stone, KL.; Williams, KR. The Protein Protocols Handbook. Totowa, NJ: Humana Press; 1996. Enzymatic digestion of proteins in solution and in SDS polyacrylamide gels.

Subra C, Laulagnier K, Perret B, Record M. Exosome lipidomics unravels lipid sorting at the level of multivesicular bodies. Biochimie. 2007; 89:205–212. [PubMed: 17157973]

van Meer G, Sprong H. Membrane lipids and vesicular traffic. Curr Opin Cell Biol. 2004; 16:373–378. [PubMed: 15261669]

van Niel G, Porto-Carreiro I, Simoes S, Raposo G. Exosomes: a common pathway for a specialized function. J Biochem. 2006; 140:13–21. [PubMed: 16877764]

Winzeler EA, Shoemaker DD, Astromoff A, Liang H, Anderson K, Andre B, et al. Functional characterization of the *S. cerevisiae* genome by gene deletion and parallel analysis. Science. 1999; 285:901–906. [PubMed: 10436161]

Wisplinghoff H, Bischoff T, Tallent SM, Seifert H, Wenzel RP, Edmond MB. Nosocomial bloodstream infections in US hospitals: analysis of 24,179 cases from a prospective nationwide surveillance study. Clin Infect Dis. 2004; 39:309–317. [PubMed: 15306996]

Woods JP. *Histoplasma capsulatum* molecular genetics, pathogenesis, and responsiveness to its environment. Fungal Genet Biol. 2002; 35:81–97. [PubMed: 11848673]

Yoneda A, Doering TL. A eukaryotic capsular polysaccharide is synthesized intracellularly and secreted via exocytosis. Mol Biol Cell. 2006; 17:5131–5140. [PubMed: 17021252]

Zancope-Oliveira RM, Reiss E, Lott TJ, Mayer LW, Deepe GS Jr. Molecular cloning, characterization, and expression of the M antigen of *Histoplasma capsulatum*. Infect Immun. 1999; 67:1947–1953. [PubMed: 10085041]

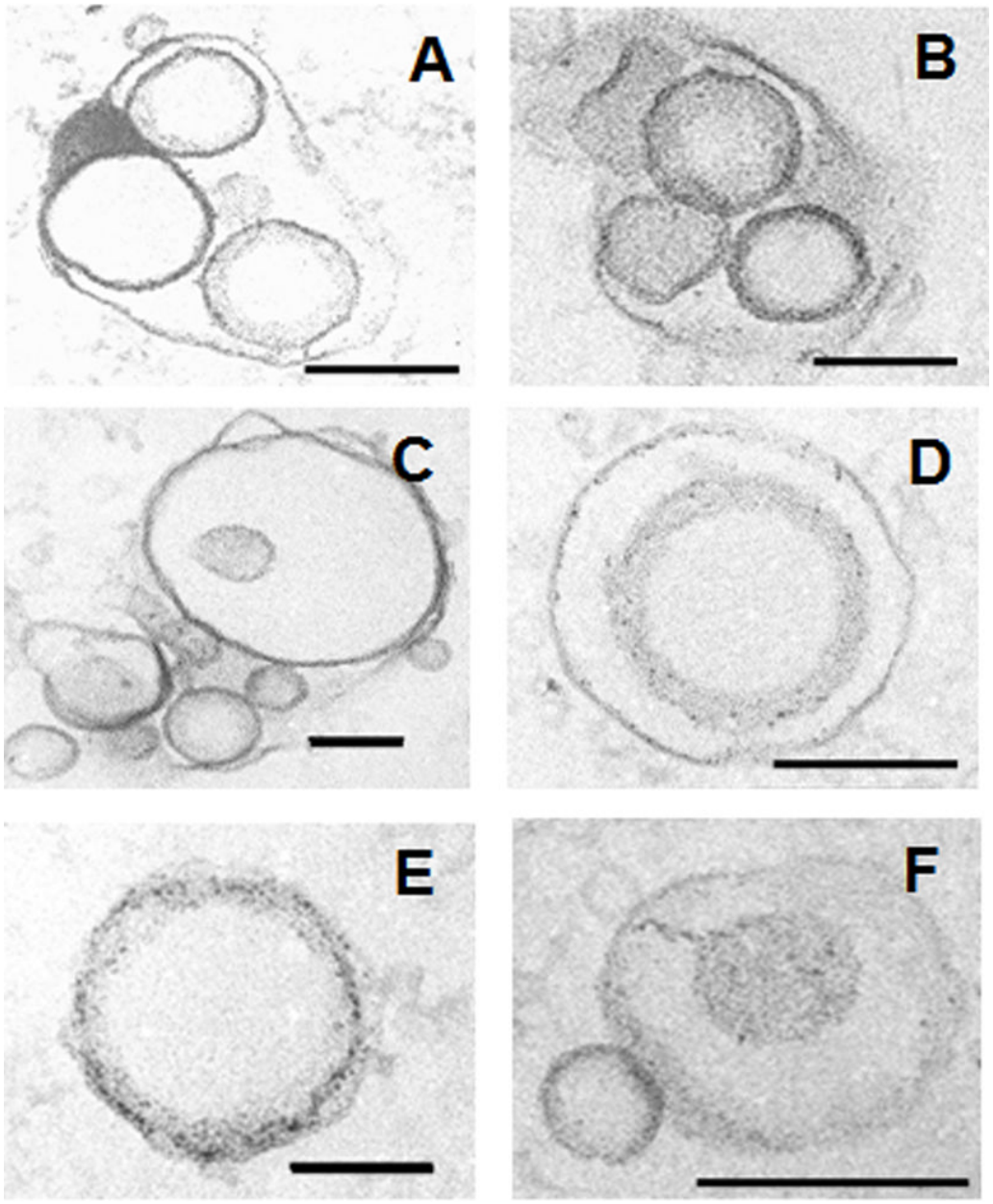

Fig.1.
TEM of extracellular vesicles obtained by ultracentrifugation of culture supernatants from *Histoplasma capsulatum* showing bilayered membranes and different profiles of electron density. Bars, 100 nm (B, C and E) and 200 nm (A, D and F).

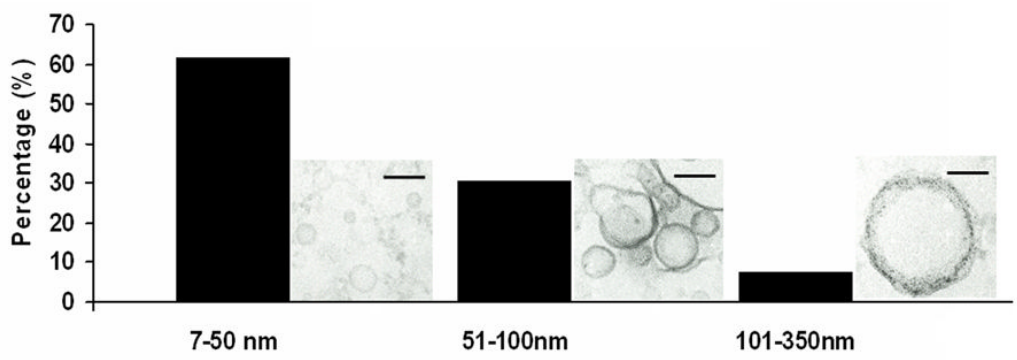

Fig.2.

Size analysis of vesicles from *H. capsulatum.* Five hundred and eight vesicles were analyzed and the size ranged from 10 to 350 nm.

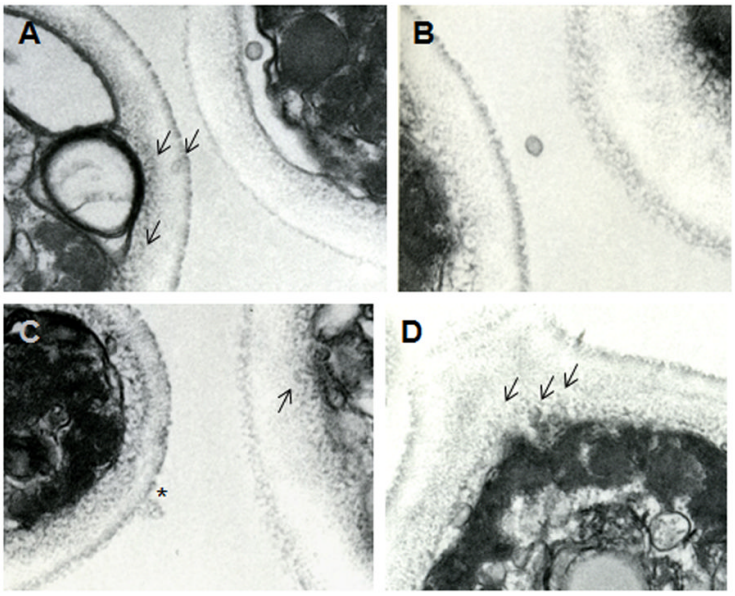

Fig.3.
Vesiclular structures were observed in association with the cell wall (A, C and D) and the extracellular environment (B).

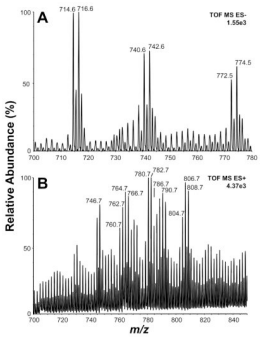

Fig.4.

Lipid analysis by mass spectrometry of *H. capsulatum* vesicular components. Total phospholipids were fractionated by silica gel 60 chromatography and analyzed by ESI-MS, in negative- (A) or positive-ion (B) mode. The ion species corresponding to major phospholipids are indicated. These ions were subjected to MS-MS analysis, allowing the identification of 18 phospholipids (Table 1; Supplemental Figure 1). *m/z*, mass to charge ratio.

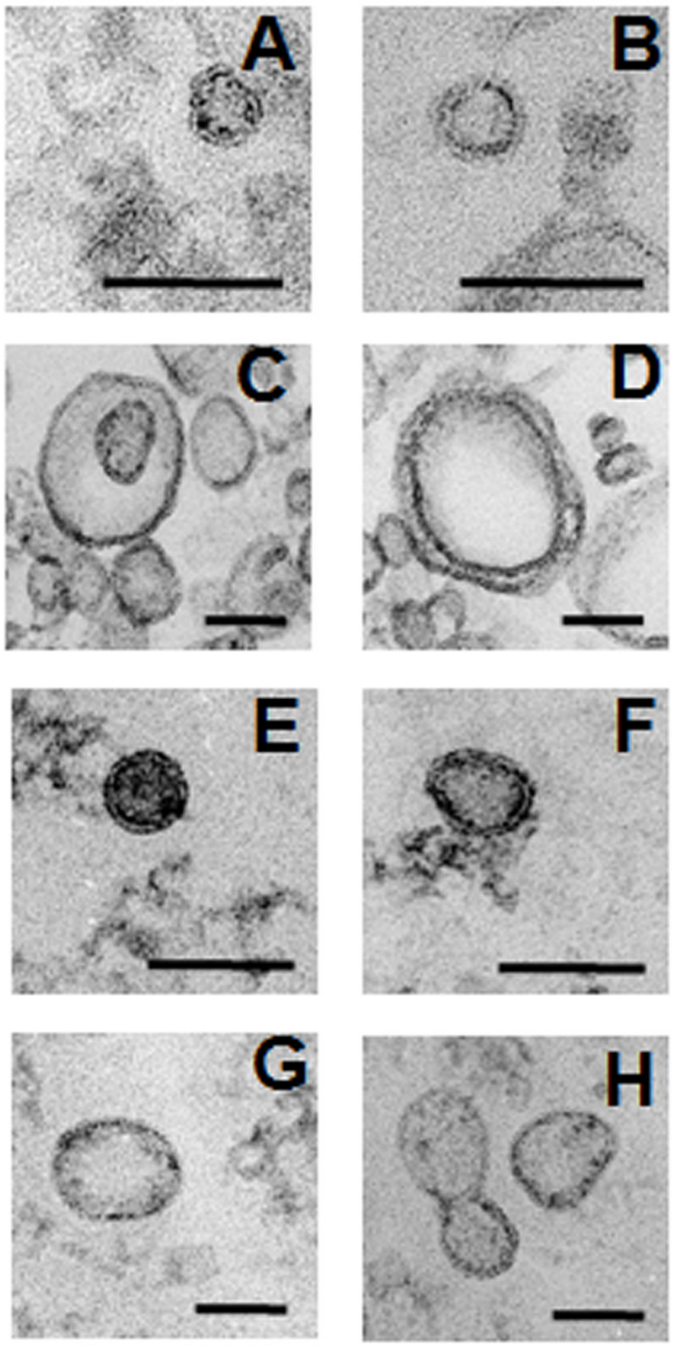

Fig. 5.

TEM of extracellular vesicles from *S. cerevisiae* (A, B), *C. parapsilosis* (C, D), *S. schenckii* (E, F) and *C. albicans* (G, H). The structures identified were similar to vesicles produced by *C. neoformans* and *H. capsulatum*. Bars 100 nm.

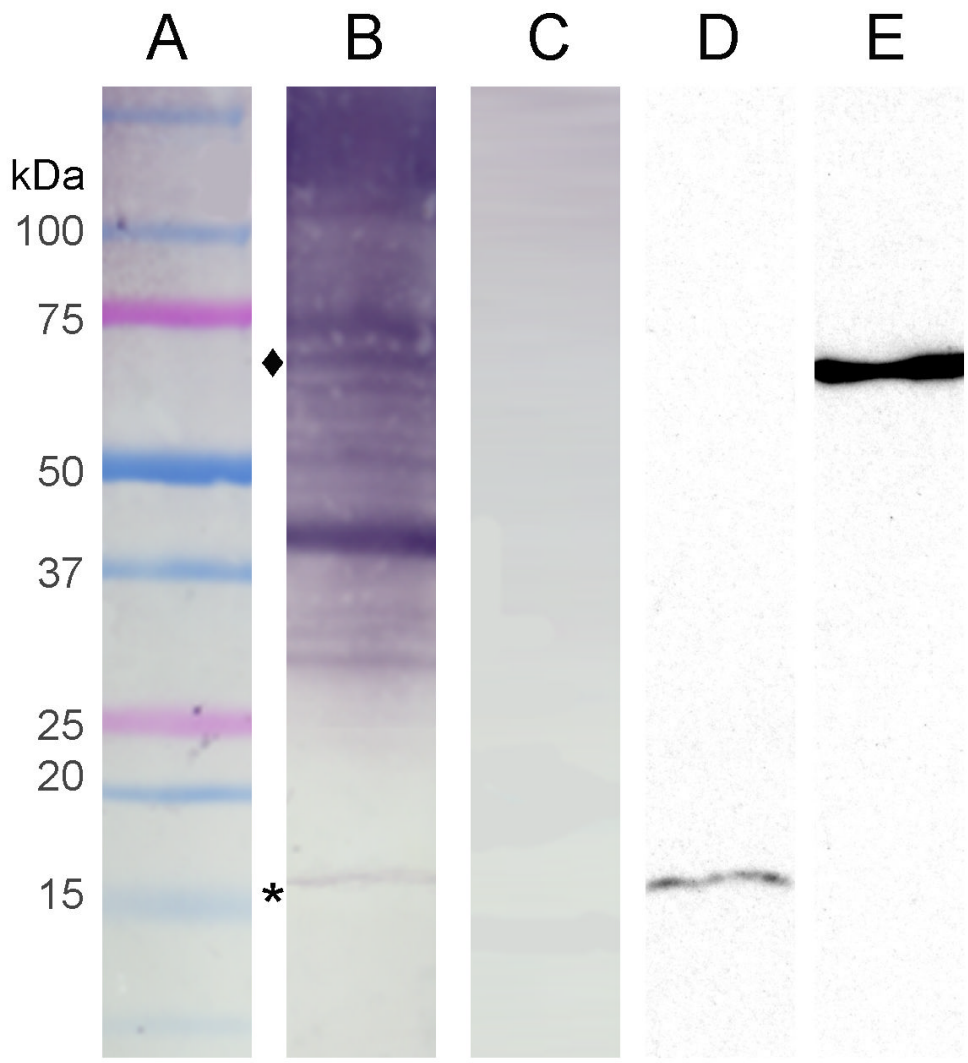

Fig. 6.

H. capsulatum vesicles contain immunoreactive proteins. Pooled serum from patients with histoplasmosis reacts with proteins from extracellular *H. capsulatum* vesicles. Lane A shows the molecular weight marker. Lane B shows *H. capsulatum* pooled hyperimmune sera reacting with extracts from *H. capsulatum* vesicles, whereas the non-immune serum in lane C does not interact with the extracted proteins. Lanes D and E demonstrate the binding of monoclonal antibodies to histone 2B (17 kDa; corresponding to *, lane B) and heat shock protein 60 (62 kDa; corresponding to ♦, lane B), respectively, in the vesicular protein preparations.

Table 1

Lipid analysis and composition of the major phospholipids from *H. capsulatum* vesicles.

MS Ion-Mode	Observed *m/z*, [ion species]	Proposed Phospholipid Composition[a]	Predicted Mass (Da)	Observed Mass (Da)
Negative	714.6, $[M - H]^-$	C16:0/C18:2-PE	715.5	715.6
Negative	716.6, $[M - H]^-$	C16:0/C18:1-PE	717.5	717.6
Negative	740.6, $[M - H]^-$	C18:2/C18:1-PE	741.5	741.6
Negative	742.6, $[M - H]^-$	C18:1/C18:1-PE	743.6	743.6
Negative	772.5, $[M - H + Na^+ + Cl^-]^+$	C16:0/C18:2-PE	715.5	715.5
Negative	774.5, $[M - H + Na^+ + Cl^-]^+$	C16:0/C18:1-PE	717.5	717.5
Positive	746.7, $[M^+ - H + Li^+]^+$	C16:0/C20:4-PE	739.5	739.7
Positive	760.7, $[M + H]^+$	C16:0/C18:2-PS	759.5	759.7
Positive	762.7, $[M + H]^+$	C16:0/C18:1-PS	761.5	761.7
Positive	764.7, $[M^+ - H + Li^+]^+$	C16:0/C18:2-PC	758.6	758.7
Positive	766.7, $[M^+ - H + Li^+]^+$	C16:0/C18:1-PC	760.6	760.7
Positive	780.7, $[M^+ - H + Na^+]^+$	C16:0/C18:2-PC	758.6	758.7
Positive	782.7, $[M^+ - H + Na^+]^+$	C16:0/C18:1-PC	760.6	760.7
Positive	786.7, $[M + H]^+$	C18:1/C18:2-PS	785.5	785.7
Positive	790.7, $[M^+ - H + Li^+]^+$	C18:1/C18:2-PC	784.6	784.7
Positive	804.7, $[M^+ - H + Na^+]^+$	C16:0/C20:4-PC	782.6	782.7
Positive	806.7, $[M^+ - H + Na^+]^+$	C18:1/C18:2-PC	784.6	784.7
Positive	808.7, $[M^+ - H + Na^+]^+$	C18:1/C18:1-PC	786.6	786.7

[a]Deduced from the MS/MS spectrum (see Supplemental Figure 1).

Cell Microbiol. Author manuscript; available in PMC 2009 August 1.

Table 2

Protein components of *H. capsulatum* vesicles.

Protein hit number	*H. capsulatum* genome database accession number	Protein identification	Function*
Chaperone-like proteins			
1	HCAG_06961.1	Heat shock protein 60, mitochondrial precursor	Chaperone
2	HCAG_01398.1	Heat shock 70 kDa protein 7	Chaperone
3	HCAG_00783.1	Heat shock protein Hsp88	Chaperone
4	HCAG_08176.1	Heat shock protein SSC1, mitochondrial precursor	Chaperone
5	HCAG_05805.1	Heat shock 70 kDa protein C precursor	Chaperone
6	HCAG_04111.1	Heat shock protein 30 kDa	Chaperone
7	HCAG_04686.1	ATP-dependent molecular chaperone HSC82	Chaperone
8	HCAG_05524.1	Hypothetical protein similar to chaperonin subunit 7	Chaperone
Cell wall architecture			
9	HCAG_06565.1	Endochitinase 1 precursor	Cell wall assembly
10	HCAG_02853.1	Hypothetical protein similar to beta-glucosidase 5	Cell wall assembly
11	HCAG_01828.1	Beta-glucosidase 4	Cell wall assembly
12	HCAG_05285.1	Beta-1,3-glucanosyltransferase 3	Cell wall assembly
13	HCAG_02309.1	Hypothetical protein similar to exo-1,3-beta-D-glucanase	Cell wall assembly
14	HCAG_08883.1	Chitin synthase B	Cell wall assembly
15	HCAG_01250.1	Endochitinase 1 precursor	Cell wall assembly
16	HCAG_04277.1	Hypothetical protein similar to mannosidase II	Cell wall assembly
17	HCAG_05925.1	Hypothetical protein similar to N-acetyl-beta-glucosaminidase	Hydrolysis of chitin oligomers
18	HCAG_00683.1	Woronin body major protein	Septal pore sealing in response to cellular damage
19	HCAG_07031.1	CPC2 protein	Putative receptor for protein kinase C in the regulation of actin cytoskeleton organization during cell wall synthesis and morphogenesis
Cell signaling			
20	HCAG_07830.1	Rab GDP-dissociation inhibitor	Regulation of the secretory pathway
21	HCAG_06999.1	Rab1a	GTP binding; small GTPase mediated signal transduction
22	HCAG_05187.1	GTP-binding nuclear protein GSP1/Ran	GTP-binding protein involved in nucleocytoplasmic transport.

Protein hit number	*H. capsulatum* genome database accession number	Protein identification	Function*
23	HCAG_05560.1	Rho GTPase	GTP binding; regulation of multiple signaling pathways
24	HCAG_01447.1	Hypothetical protein similar to GTP binding protein	GTP binding
25	HCAG_04173.1	14-3-3 protein epsilon (308 aa)	Adapter protein implicated in the regulation of a large spectrum of both general and specialized signaling pathways
26	HCAG_04527.1	14-3-3 family protein ArtA	Cell signaling
27	HCAG_04840.1	GTP-binding protein sarA	Regulation of transport from the endoplasmic reticulum to the Golgi apparatus
Sugar metabolism			
28	HCAG_08808.1	Phosphoglucomutase	Breakdown and synthesis of glucose
29	HCAG_03803.1	Hydroxymethylglutaryl-CoA lyase, mitochondrial precursor	Ketogenesis, production of acetyl-CoA and from (S)-3-hydroxy-3-methylglutaryl-CoA
30	HCAG_06184.1	Isocitrate lyase	Glyoxylate cycle; production of L-malate from isocitrate
31	HCAG_02260.1	3-isopropylmalate dehydrogenase A	Oxidation of 3-carboxy-2-hydroxy-4-methylpentanoate (3-isopropylmalate) to 3-carboxy-4-methyl-2-oxopentanoate
32	HCAG_07619.1	Pyruvate dehydrogenase E1 component beta subunit, mitochondrial precursor	Conversion of pyruvate to acetyl-CoA and CO
33	HCAG_04910.1	Glyceraldehyde-3-phosphate dehydrogenase	Glycolysis; pyruvate formation from D-glyceraldehyde 3-phosphate
34	HCAG_06981.1	Citrate synthase, mitochondrial precursor	Tricarboxylic acid cycle
35	HCAG_00638.1	Transaldolase	Balance of metabolites in the pentose-phosphate pathway
36	HCAG_04227.1	Hypothetical protein similar to pyruvate carboxylase	Tricarboxylic acid cycle
37	HCAG_03969.1	Malate dehydrogenase, mitochondrial precursor	Conversion of malate into oxaloacetate
38	HCAG_08720.1	Mannitol-1-phosphate dehydrogenase	Mannitol synthesis
39	HCAG_05084.1	Hypothetical protein similar to malate synthase 2	2-Isopropylmalate formation from the condensation of the acetyl group of acetyl-CoA with 3-methyl-2-oxobutanoate
40	HCAG_00626.1	Sorbitol utilization protein SOU1	NADP dependent reduction of L-sorbose to D-glucitol
41	HCAG_00064.1	Hypothetical protein similar to phosphoacetylglucosamine mutase	Interconverts N-acetylglucosamine-6-P and N-acetylglucosamine -1-P
42	HCAG_03323.1	Hypothetical protein similar to fumarate reductase	Unidirectional fumarate reduction
43	HCAG_08493.1	Fumarate hydratase class II	Conversion of malate into fumarate, tricarboxylic acid cycle
44	HCAG_03385.1	Phosphoglycerate kinase	Conversion of 3-phospho-D-glycerate into 3-phospho-D-glyceroyl phosphate; glycolysis.
45	HCAG_07781.1	Hypothetical protein similar to CDC19 *Also known as:* Pyruvate kinase 1	Glycolysis, conversion of pyruvate to phosphoenolpyruvate

Protein hit number	*H. capsulatum* genome database accession number	Protein identification	Function*
46	HCAG_05884.1	Hypothetical protein similar to 6-Phosphogluconate dehydrogenase	Formation of D-ribulose 5-phosphate; pentose phosphate pathway
47	HCAG_08202.1	Glucose-6-phosphate isomerase	Conversion of D-glucose 6-phosphate into D-fructose 6-phosphate; glycolysis
48	HCAG_01552.1	Mannose-1-phosphate guanyltransferase	Synthesis of GDP-mannose; protein glycosylation
49	HCAG_04139.1	Phosphomannomutase	Synthesis of the GDP-mannose
50	HCAG_06317.1	Succinate dehydrogenase flavoprotein subunit, mitochondrial precursor	Tricarboxylic acid cycle
51	HCAG_00010.1	Fructose-bisphosphate aldolase	Carbohydrate degradation; glycolysis
52	HCAG_07697.1	Succinyl-CoA ligase beta-chain, mitochondrial precursor	Tricarboxylic acid cycle
53	HCAG_03263.1	Succinate dehydrogenase iron-sulfur protein, mitochondrial precursor	Tricarboxylic acid cycle
54	HCAG_05090.1	2-methylcitrate synthase, mitochondrial precursor	Propionate catabolism; 2-methylcitric acid cycle.
55	HCAG_01535.1	2-oxoglutarate dehydrogenase E1 component, mitochondrial precursor	Conversion of 2-oxoglutarate to succinyl-CoA and CO2; tricarboxylic acid cycle.
56	HCAG_04416.1	UDP-N-acetylglucosamine pyrophosphorylase	*De novo* biosynthetic pathway for UDP-GlcNAc
57	HCAG_03522.1	Dihydrolipoyllysine-residue succinyltransferase component of 2-oxoglutarate dehydrogenase complex, mitochondrial precursor	Conversion of 2-oxoglutarate to succinyl-CoA and CO2; tricarboxylic acid cycle.
58	HCAG_05266.1	Aconitate hydratase, mitochondrial precursor	Conversion of citrate to isocitrate; tricarboxylic acid cycle.
59	HCAG_06641.1	Hypothetical protein similar to UDP-galactopyranose mutase	Conversion of UDP-galactopyranose into UDP-galactofuranose
60	HCAG_02511.1	Triose phosphate isomerase	Carbohydrate degradation; glycolysis
61	HCAG_03191.1	Glucokinase	Phosphorylation of aldohexoses and glucose uptake
62	HCAG_03322.1	Fructose-1,6-bisphosphatase	Gluconeogenesis; D-fructose 6-phosphate formation
63	HCAG_05681.1	Phosphoenolpyruvate carboxykinase	Formation of phosphoenolpyruvate, gluconeogenesis
Lipid metabolism			
64	HCAG_00413.1	Farnesyl pyrophosphate synthetase	Isoprene biosynthesis, sterol biosynthesis.
65	HCAG_01596.1	Hypothetical protein similar to 3-ketoacyl-CoA thiolase B	Formation of 3-oxoacyl-CoA, fatty acid beta-oxidation
66	HCAG_08039.1	Hypothetical protein similar to peroxisomal hydratase-dehydrogenase-epimerase	Beta-oxidation pathway for fatty acids; converts trans-2-enoyl-CoA via D-3-hydroxyacyl-CoA to 3-ketoacyl-CoA.
67	HCAG_04933.1	Hypothetical protein similar to ATP-citrate-lyase	Cleavage of citrate to yield acetyl CoA, oxaloacetate, ADP, and orthophosphate; fatty acid biosynthesis
68	HCAG_01606.1	Acetyl-coenzyme A synthetase 2	Acetyl-CoA synthesis
69	HCAG_08621.1	Acetyl-CoA acetyltransferase	Short-chain fatty acid metabolism
70	HCAG_04934.1	ATP-citrate synthase subunit 1	Formation of cytosolic acetyl-CoA, fatty acid synthesis

Protein hit number	*H. capsulatum* genome database accession number	Protein identification	Function*
71	HCAG_07725.1	3-hydroxybutyryl-CoA dehydrogenase	Formation of an hydroxyacyl-CoA, fatty acid oxidation
72	HCAG_07637.1	Fatty acid synthase beta subunit dehydratase	Fatty acid biosynthesis
Amino acid and protein metabolism			
73	HCAG_06019.1	Ubiquitin	Pos translational protein modification
74	HCAG_03166.1	Ubiquitin-conjugating enzyme E2-17 kDa	Catalyzes the attachment of ubiquitin to other proteins
75	HCAG_05565.1	5-methyltetrahydropteroyltriglutamate--homocysteine methyltransferase (764 aa)	Methionine formation
76	HCAG_05651.1	Glutamate dehydrogenase	N-acetyl-L-glutamate 5-phosphate formation; L-arginine biosynthesis
77	HCAG_07571.1	Glycine dehydrogenase, mitochondrial precursor	Degradation of glycine
78	HCAG_06102.1	Aspartate aminotransferase, mitochondrial precursor	Conversion of L-aspartate + 2-oxoglutarate into oxaloacetate + L-glutamate.
79			
80	HCAG_09000.1	Delta-1-pyrroline-5-carboxylate dehydrogenase, mitochondrial precursor	L-glutamate biosynthesis
81	HCAG_00677.1	Isovaleryl-CoA dehydrogenase, mitochondrial precursor	Leucine catabolism
82	HCAG_08890.1	Ketol-acid reductoisomerase, mitochondrial precursor	L-isoleucine biosynthesis
83	HCAG_00676.1	Methylcrotonoyl-CoA carboxylase beta chain, mitochondrial precursor	Leucine catabolism
84	HCAG_00029.1	Mitochondrial methylglutaconyl-CoA hydratase	Leucine catabolism
85	HCAG_04215.1	Peptidyl-prolyl cis-trans isomerase A	Protein folding
86	HCAG_04485.1	Peptidyl-prolyl cis-trans isomerase	Protein folding
87	HCAG_08833.1	Peptidyl-prolyl cis-trans isomerase	Protein folding
88	HCAG_07972.1	FK506-binding protein	Protein folding
89	HCAG_00035.1	Arginase	Formation of urea from arginine
90	HCAG_02357.1	Histidinol dehydrogenase	L-histidine biosynthesis
91	HCAG_06901.1	Malate dehydrogenase	Oxidation of 3-carboxy-2-hydroxy-4-methylpentanoate (3-isopropylmalate) to 3-carboxy-4-methyl-2-oxopentanoate
92	HCAG_08058.1	Enoyl-CoA hydratase, mitochondrial precursor	conversion of 3-methylglutaconyl-CoA to 3-hydroxy-3-methylglutaryl-CoA, leucine metabolism
93	HCAG_03650.1	NAD-specific glutamate dehydrogenase	Amino acid catabolism; oxoglutarate production
94	HCAG_07418.1	Serine hydroxymethyltransferase	Interconversion of serine and glycine
95	HCAG_05988.1	Hypothetical protein similar to elongation factor 2	Protein biosynthesis; polypeptide chain elongation

Protein hit number	*H. capsulatum* genome database accession number	Protein identification	Function*
96	HCAG_08798.1	Translation elongation factor 1-alpha	Protein biosynthesis; polypeptide chain elongation
97	HCAG_04297.1	Hypothetical protein similar to aspartyl aminopeptidase	Release of an N-terminal aspartate or glutamate from a peptide, with a preference for aspartate
98	HCAG_03371.1	Adenosylhomocysteinase	Homocysteine biosynthesis
99	HCAG_01212.1	Histoplasma capsulatum sulfate adenylyltransferase	Biosynthesis of sulfur-containing amino acids
100	HCAG_04206.1	Eukaryotic translation initiation factor 2 gamma subunit	Protein synthesis
101	HCAG_04356.1	eukaryotic translation initiation factor 3 39 kDa subunit	Protein synthesis
102	HCAG_00267.1	Hypothetical protein similar to eukaryotic translation initiation factor 3 subunit 7	Protein synthesis
103	HCAG_00678.1	Hypothetical protein similar to 3-methylcrotonyl-CoA carboxylase biotin-containing subunit	Catabolism of leucine and isovalerate
104	HCAG_08678.1	Aspartate aminotransferase	Oxaloacetate production, amino acid metabolism
105	HCAG_03630.1	Disulfide-isomerase precursor	Rearrangement of -S-S- bonds in proteins
106	HCAG_06021.1	Translation initiation factor 5A-2	Protein synthesis
107	HCAG_00131.1	Nuclear transport factor 2	Protein synthesis
108	HCAG_00635.1	Subtilase-type proteinase psp3 precursor	Peptidase
109	HCAG_07805.1	Argininosuccinate lyase	Fumarate and L-arginine synthesis
Ribosomal proteins			
110	HCAG_01850.1	60S ribosomal protein L10a	Ribosomal protein
111	HCAG_00055.1	60S ribosomal protein L27-A	Ribosomal protein
112	HCAG_04185.1	60S ribosomal protein L36	Ribosomal protein
113	HCAG_02703.1	60S acidic ribosomal protein P2	Ribosomal protein
114	HCAG_04231.1	60S ribosomal protein L11-1	Ribosomal protein
115	HCAG_03695.1	60S ribosomal protein L10-B	Ribosomal protein
116	HCAG_07463.1	60S ribosomal protein L18-B	Ribosomal protein
117	HCAG_08515.1	60S ribosomal protein L2	Ribosomal protein
118	HCAG_03923.1	60S ribosomal protein L3	Ribosomal protein
119	HCAG_08444.1	60S ribosomal protein L5	Ribosomal protein
120	HCAG_00468.1	60S ribosomal protein L4-A	Ribosomal protein
121	HCAG_02430.1	40S ribosomal protein S5	Ribosomal protein

Protein hit number	*H. capsulatum* genome database accession number	Protein identification	Function*
122	HCAG_06613.1	40S ribosomal protein S7	Ribosomal protein
123	HCAG_06914.1	40S ribosomal protein S3A	Ribosomal protein
124	HCAG_07773.1	40S ribosomal protein S11	Ribosomal protein
125	HCAG_06308.1	40S ribosomal protein S12	Ribosomal protein
126	HCAG_01666.1	ribosomal protein S6	Ribosomal protein
127	HCAG_08667.1	40S ribosomal protein S18	Ribosomal protein
128	HCAG_02272.1	40S ribosomal protein S22	Ribosomal protein
129	HCAG_07237.1	ribosomal protein S4	Ribosomal protein
130	HCAG_07961.1	ribosomal protein S5	Ribosomal protein
131	HCAG_03504.1	ribosomal protein L22	Ribosomal protein
132	HCAG_08821.1	ribosomal protein S20	Ribosomal protein
133	HCAG_04498.1	ribosomal protein S21e	Ribosomal protein
134	HCAG_06425.1	ribosomal protein L32	Ribosomal protein
135	HCAG_00214.1	Hypothetical protein similar to ribosomal protein S3	Ribosomal protein
136	HCAG_03415.1	Hypothetical protein similar to ribosomal protein L35	Ribosomal protein
137	HCAG_04856.1	ribosomal protein P0	Ribosomal protein
138	HCAG_07708.1	Hypothetical protein similar to ribosomal protein L13	Ribosomal protein
139	HCAG_06198.1	Hypothetical protein similar to QDE2 protein	Structural constituent of ribosome
140	HCAG_03694.1	Large ribosomal subunit protein L30	Ribosomal protein
Proteasome components			
141	HCAG_04090.1	Proteasome component C1	Proteasome Component
142	HCAG_05739.1	Proteasome component Y13	Proteasome Component
143	HCAG_04101.1	Proteasome component C5	Proteasome Component
144	HCAG_00053.1	Proteasome component C7-alpha	Proteasome Component
145	HCAG_07121.1	Proteasome component PUP2	Proteasome Component
146	HCAG_03737.1	Proteasome component Pup1	Proteasome Component
147	HCAG_04198.1	Proteasome component PRE1	Proteasome Component
148	HCAG_05910.1	Proteasome component PRE2 precursor	Proteasome Component

Protein hit number	*H. capsulatum* genome database accession number	Protein identification	Function*
149	HCAG_06342.1	Proteasome component PRE3 precursor	Proteasome Component
150	HCAG_04107.1	Proteasome component PRE4	Proteasome Component
151	HCAG_08215.1	Proteasome component PRE5	Proteasome Component
152	HCAG_00347.1	Proteasome component PRE6	Proteasome Component
153	HCAG_03939.1	Proteasome component Pre8	Proteasome Component
Nuclear proteins			
154	HCAG_03885.1	Histone H4.2	DNA assembly
155	HCAG_03524.1	Histone H2A	DNA assembly
156	HCAG_03525.1	Histone H2B	DNA assembly, cell surface component in *H. capsulatum*
157	HCAG_02608.1	Guanine nucleotide-binding protein beta subunit	Nucleotide binding
158	HCAG_01433.1	Adenylosuccinate lyase	Purine metabolism; AMP biosynthesis via de novo pathway
159	HCAG_04273.1	eukaryotic initiation factor 4A	ATP-dependent RNA helicase
160	HCAG_06523.1	Curved DNA-binding protein 42 kDa protein	DNA-binding protein.
161	HCAG_00544.1	Nucleoside-diphosphate kinase	Phosphate exchange between different nucleoside diphosphates
162	HCAG_02553.1	Small nuclear ribonucleoprotein Sm D2	Pre-mRNA splicing
163	HCAG_01986.1	Poly(A)+ RNA export protein	Nuclear mRNA export
164	HCAG_00018.1	Nucleosome binding protein	Nucleosome binding
Cell growth/division			
165	HCAG_00717.1	Hypothetical protein similar to septin-1	Cytokinesis
166	HCAG_02452.1	Cell division cycle protein 48	Regulation of cell growth
167	HCAG_06283.1	AAC1 protein	Spore germination
168	HCAG_08831.1	Formamidase	Formamide hydrolysis with the production of ammonia, to be used as nitrogen source
Plasma membrane proteins			
169	HCAG_06977.1	Plasma membrane ATPase	Hydrogen-exporting ATPase activity, phosphorylative mechanism
170	HCAG_06935.1	Hypothetical protein similar to aminopeptidase B	Single-pass type II membrane protein
171	HCAG_07210.1	Glycolipid-anchored surface protein 5 precursor	Cell membrane lipid anchor
Cytoskeleton proteins			
172	HCAG_04706.1	ARP2/3 complex 34 kDa subunit	Regulation of actin polymerization

Protein hit number	*H. capsulatum* genome database accession number	Protein identification	Function*
173	HCAG_04115.1	Arp2/3 complex chain sop2	Regulation of actin polymerization
174	HCAG_00848.1	Arp2/3 complex subunit	Regulation of actin polymerization
175	HCAG_08210.1	Actin	Cytoskeleton assembly
Anti-oxidant proteins			
176	HCAG_06210.1	Thiol-specific antioxidant protein	Antioxidant defense
177	HCAG_08064.1	Catalase B	Antioxidant defense
178	HCAG_03448.1	Superoxide dismutase, mitochondrial precursor	Antioxidant defense
179	HCAG_01543.1	Superoxide dismutase, mitochondrial precursor	Antioxidant defense
180	HCAG_07098.1	Ascorbate peroxidase	Antioxidant defense
181	HCAG_08190.1	Oxidoreductase 2-nitropropane dioxygenase	Antioxidant defense
Miscellaneous			
182	HCAG_03815.1	ATP synthase subunit 5, mitochondrial precursor	Purine metabolism; AMP biosynthesis via de novo pathway
183	HCAG_06944.1	ATP synthase beta chain, mitochondrial precursor	Proton-dependent ATP production
184	HCAG_00404.1	Vacuolar ATP synthase catalytic subunit A	ATP synthesis
185	HCAG_06929.1	NADH-ubiquinone oxidoreductase 78 kDa subunit, mitochondrial precursor	Core subunit of the mitochondrial membrane respiratory chain NADH dehydrogenase
186	HCAG_04307.1	Inorganic pyrophosphatase	Phosphate supply
187	HCAG_00437.1	Hypothetical protein similar to cytochrome-c oxidase chain VI precursor	Mitochondrial electron transport
188	HCAG_05938.1	Cytochrome c	Mitochondrial electron transport
189	HCAG_02342.1	Mitochondrial processing peptidase beta subunit	Mitochondrial protein processing
190	HCAG_02570.1	Cytochrome P450 55A3	Electron transfer component.
191	HCAG_04096.1	Allergen Asp f 4	Induction of allergic reactions
192	HCAG_02813.1	ATP synthase alpha chain isoform, mitochondrial precursor	Hydrogen ion transporting ATP synthase activity
193	HCAG_06539.1	Hypothetical protein similar to succinate:fumarate antiporter	Transmembrane transport
194	HCAG_03543.1	Glutamate carboxypeptidase	Hydrolysis of reduced and non-reduced folates to pteroates and L-glutamate
195	HCAG_05000.1	Transketolase 1	Assimilation of formaldehyde
196	HCAG_06026.1	Polyadenylate-binding protein	Binding of the poly(A) tail of mRNA
197	HCAG_04999.1	Spermidine synthase	Amine and polyamine biosynthesis; spermidine biosynthesis

Protein hit number	*H. capsulatum* genome database accession number	Protein identification	Function *
198	HCAG_02994.1	Pyridoxal biosynthesis lyase pdxS	Pyridoxal phosphate production
199	HCAG_02035.1	Imidazole glycerol phosphate synthase hisHF	Synthesis of Imidazole glycerol phosphate
200	HCAG_07004.1	O-acetylhomoserine	Catalysis of trans-sulfuration.
201	HCAG_08367.1	Aldehyde dehydrogenase	Aldehyde oxidation
202	HCAG_03605.1	Zinc-binding dehydrogenase	Ethanol metabolism
203	HCAG_08561.1	Alcohol dehydrogenase I	Interconversion between alcohols and aldehydes or ketones
204	HCAG_07206.1	S-(hydroxymethyl)glutathione dehydrogenase	Interconversion between alcohols and aldehydes or ketones
205	HCAG_05094.1	2-Methylcitrate dehydratase	dehydration of 2-methylcitrate to 2-methyl-cis-aconitate
206	HCAG_03008.1	Sulfur metabolite repression control protein C	Regulation of sulfur metabolism

* Biological functions of the proteins detected by proteomics were obtained from the ExPASy Proteomics Server (http://ca.expasy.org/). Proteins with unknown functions were also identified, but are not present in this table. For detailed information, see Supplemental material.

Table 3

Distribution of the identified *H. capsulatum* vesicle proteins according to their functions.

Protein association	Percent total (%)
Amino acid/protein metabolism	37
Sugar metabolism	36
Ribosomal	31
Proteasome component	13
Nuclear	11
Cell wall architecture	11
Lipid metabolism	9
Cell signaling	8
Chaperone-like	8
Anti-oxidant	6
Cytoskeletal	4
Cell growth/division	4
Plasma membrane	3
Miscellaneous	25